Electrocatalysis (2014) 5:310–317
DOI 10.1007/s12678-014-0196-z

Direct Dimethyl Ether Fuel Cell with Much Improved Performance

Qing Li · Gang Wu · Christina M. Johnston · Piotr Zelenay

Published online: 4 April 2014
© The Author(s) 2014. This article is published with open access at Springerlink.com

Abstract Due to several apparent advantages over methanol, dimethyl ether (DME) has been viewed as a promising alternative fuel for direct fuel cell technology. Similar to methanol, DME oxidation requires a surface oxidant, such as OH, for the removal of adsorbed CO. Consequently, the reaction occurs at much faster rates on binary PtRu catalysts than Pt alone. In this work, PtRu catalysts with a wide variety of Pt-to-Ru ratios were systematically studied in the direct DME fuel cell (DDMEFC) operating at 80 °C. A $Pt_{50}Ru_{50}$ catalyst was found to perform the best at high and middle voltages, while a $Pt_{80}Ru_{20}$ catalyst performed best at low voltages. DDMEFC operation conditions, such as DME flow rate, anode back pressure, DME-to-water molar ratio, and membrane thickness, were also studied in order to maximize the cell performance. A maximum power density of 0.12 W cm^{-2} obtained in this work exceeds the highest reported DME performance. In comparison with the direct methanol fuel cell (DMFC), the optimized DDMEFC performs better at cell voltages higher than 0.55 and 0.49 V with feed concentrations of methanol of 0.5 and 1.0 M, respectively.

Keywords Dimethyl ether · DME · Electrooxidation · PtRu catalysts · Direct dimethyl ether fuel cell

Introduction

The rapid development of portable electronic devices, such as mobile phones, notebooks, and digital cameras, has significantly increased the demand for high-output power sources. The direct methanol fuel cell (DMFC) has long been viewed as a highly promising power source for such devices thanks to the high energy density of methanol and no requirement for fuel reforming. However, the DMFC performance is limited by various factors, including the slow kinetics of methanol oxidation, crossover of methanol and ruthenium from the anode to the cathode side of the cell, and safety concerns over the methanol fuel itself.

Dimethyl ether (DME), a widely used gas for aerosol propulsion, solvents, and coolants, has been investigated in the last decade as an alternative fuel for direct-feed fuel cells [1]. Complete oxidation of one DME molecule to CO_2 releases 12 electrons and, similar to the oxidation of methanol, does not require a C–C bond scission:

$$CH_3OCH_3 + 3H_2O \rightarrow 2CO_2 + 12H^+ + 12e \quad (1)$$

The energy density of DME is higher than that of methanol (8.2 vs. 6.1 kWh kg^{-1}), and the theoretical open-cell voltage of the direct DME fuel cell (DDMEFC) is close to that of the DMFC (1.18 vs. 1.21 V at 25 °C). Because of a lower value of the dipole moment, the DME fuel crossover is less than methanol, mitigating the negative impact on the cathode due to mixed potentials [2, 3]. DME is also less toxic than methanol and can be conveniently stored and transported using existing infrastructure and technologies. A comparison of selected physicochemical properties of DME and methanol is shown in Table 1.

The DDMEFC has been studied to a much lesser degree than other direct-feed fuel cells that use methanol, ethanol, and formic acid as fuels. A summary of the DDMEFC development can be found in a recent review by Serov et al. [4]. To date, the mechanism of DME oxidation has not been fully clarified yet. Traces of methanol and formic acid were detected in the DDMEFC anode exhaust by Müller et al. [2] and by Tsutsumi et al. [5], respectively. As a result, different DME electrooxidation mechanisms were proposed. A possible mechanism of DME oxidation on Pt was proposed by Müller et al. [2]:

Q. Li · G. Wu · C. M. Johnston · P. Zelenay (✉)
Materials Physics and Applications Division, Los Alamos National Laboratory, Los Alamos, NM 87545, USA
e-mail: zelenay@lanl.gov

Table 1 Comparison of selected physicochemical properties of DME and methanol

	Density (g $mL^{-1)}$	Boiling point (°C)	Dipole moment (D)	Energy density (kWh kg^{-1})
DME	1.97	−24	1.30	8.2
Methanol	0.79	65	1.69	6.1

$$CH_3OCH_3 + Pt \rightarrow Pt(C–O–CH_3)_{ad} + 3e + 3H^+ \quad (2)$$

$$Pt(C–O–CH_3)_{ad} + H_2O \rightarrow Pt(HCO)_{ads} + CH_3OH \quad (3)$$

$$Pt(HCO)_{ad} \rightarrow Pt(CO)_{ad} + H^+ + e \quad (4)$$

$$Pt(HCO)_{ad} + Pt–OH \rightarrow 2Pt + CO_2 + 2H^+ + 2e \quad (5)$$

$$Pt(CO)_{ad} + Pt–OH \rightarrow 2Pt + CO_2 + H^+ + e \quad (6)$$

Several DME adsorption species, such as $(CH_3OC–)_{ad}$, CO_L (linearly bonded CO), and CO_B (bridge-bonded CO), were detected by in situ infrared (IR) spectroscopy [6–9]. The fractional coverage of CO_L was found to increase with potential from 0.1 to 0.4 V, reaching more than 0.5 in the potential range from 0.3 to 0.5 V [8]. The oxidation of CO_{ads} is most likely the rate-determining step (RDS) of DME oxidation at low potentials. Similar to methanol oxidation, bimetallic platinum-based alloys capable of mitigating the poisonous effect of CO_{ads} on Pt were found to be the most effective in DME oxidation. Liu et al. [10] investigated the DME oxidation on a series of PtM/C (M=Ru, Sn, Mo, Cr, Ni, Co, W) and Pt/C electrocatalysts and demonstrated that PtRu/C shows the best electrocatalytic activity and the highest tolerance to the chemisorbed species at low potentials, specially below 0.55 V (at 50 °C). In the DDMEFC, performance of PtRu was found to be superior to that of Pt, PtPd [11], and PtSn [12].

This work represents the first systematic study of unsupported PtRu catalysts with different atomic compositions ($Pt_{90}Ru_{10}$, $Pt_{80}Ru_{20}$, $Pt_{67}Ru_{33}$, $Pt_{50}Ru_{50}$, $Pt_{40}Ru_{60}$, and $Pt_{34}Ru_{66}$) in the DDMEFC anode at 80 °C. The role of Ru in these binary electrocatalysts is discussed based on the experimental results. Also studied is the effect of fuel cell operation conditions, such as the DME flow rate, anode back pressure, DME-to-water molar ratio, and membrane thickness. These are important factors in maximizing the DDMEFC performance and bringing it closer to the performance of a DMFC.

Experimental Section

MEA Preparation

The membrane-electrode assemblies (MEAs) were fabricated using Nafion® 117 and Nafion® 212 membranes and catalyst inks. Unsupported $Pt_{90}Ru_{10}$, $Pt_{80}Ru_{20}$, $Pt_{67}Ru_{33}$, $Pt_{50}Ru_{50}$, $Pt_{40}Ru_{60}$, and $Pt_{34}Ru_{66}$ (Johnson Matthey) and Pt (Johnson Matthey) catalysts were used for anode and cathode catalyst layers, respectively. Catalyst inks were prepared by ultrasonically mixing appropriate amounts of catalyst powders with water (Millipore, 18 MΩ cm^{-1}) and 5 % Nafion® suspension in alcohols (Ion Power, Inc) for 90 s. The catalyst ink was then directly applied to the membrane at 75 °C and dried for 30 min. The catalyst loadings (total metals) were 6.0 and 4.0 mg cm^{-2} at the anode and cathode, respectively. Carbon paper-based GDL 25 BC and GDL 25 BL (SGL Group) were used correspondingly at the anode and cathode. The MEA geometric active area was 5 cm^2.

Fuel Cell Testing

DDMEFC and DMFC tests were carried out in a single fuel cell using a commercial test station (Fuel Cell Technologies, Inc.). The MEA was sandwiched between two graphite serpentine flow fields. The flow fields were placed in between two aluminum compression plates, which were held together with a set of eight retaining bolts positioned around the periphery of the cell. The cell was operated at 80 °C. DME gas (99 % purity, Aldrich) was bubbled through the humidity bottles and then fed to the anode. Before switching to the DDMEFC operating mode, the cell was first operated on H_2 to assure adequate performance of the cathode. The hydrogen/air fuel cell performance was recorded after a 2-h break-in at 0.7 V using fully humidified gases at a back pressure of ca. 1.4 bar (ca. 2.2 bar absolute at the Los Alamos altitude). To measure the high-frequency resistance (HFR), a sinusoidal voltage perturbation between 2 and 10 kHz (chosen to minimize capacitance) was applied to the fuel cell load. During DMFC testing, methanol was pumped through the anode flow field at a flow rate of 1.8 mL min^{-1}, using a high-pressure liquid chromatography pump (Shimadzu LC-10AS). To determine the fuel crossover, nitrogen was fed into the cathode, and the cell was operated in a driven mode using an external power supply (HP 6061A, Hewlett-Packard, USA). All results reported below are the average from three independent experiments.

Electrochemical Measurements

As for electrochemical ("half-cell") measurements, catalyst powders were ultrasonically dispersed in a mixture of Millipore® water and 5 % Nafion® suspension in alcohols (Ion Power, Inc) for 30 min. Fifteen microliters of the

suspension was then quantitatively transferred to the surface of a polished glassy carbon working electrode with a geometric area of 0.196 cm^2 (controlled Pt loading of 60 μg cm^{-2}). The electrochemical measurements were performed using a CHI Electrochemical Station (model 750b) in a conventional three-electrode cell. A platinized platinum electrode immersed in the supporting electrolyte (0.1 M $HClO_4$) saturated with forming gas (6 % H_2 in N_2) was used as a reference electrode. All measured working electrode potentials were later converted to the reversible hydrogen electrode (RHE) scale. A graphite rod was used as the counter electrode. The working electrode was electrochemically cleaned under a nitrogen atmosphere in the electrolyte between 0.05 and 1.2 V at a scan rate of 50 mV s^{-1} until a steady-state voltammogram was obtained. DME gas was bubbled through the 0.1 M $HClO_4$ solution at ambient pressure for ca. 3 min to form a saturated solution with a saturation DME concentration of 0.81 M (estimated from the sea level solubility DME in water of 1.05 M [6], subsequently corrected for the altitude of Los Alamos using Henry's law). All experiments were carried out at room temperature.

Results and Discussion

DDMEFC Tests with Different PtRu Catalysts

Six PtRu catalysts were evaluated at the DDMEFC anode. The fuel cell voltage and HFR as a function of the current density are plotted in Fig. 1. $Pt_{50}Ru_{50}$ shows the best overall performance in the high- and middle-voltage ranges, and $Pt_{80}Ru_{20}$ is the best performer at low cell voltages (high anode overpotentials).

The DDMEFC open-cell voltage (OCV) and current density at different fuel cell voltage values are shown as a function of the Pt content in PtRu catalysts in panels a and b, respectively, of Fig. 2. Higher OCV values are measured with Ru-rich catalysts, which also show better performance at high fuel cell voltages, where the performance is controlled by the kinetics of the anode process. Pt-rich catalysts perform better at low voltages, near the peak of power density. This effect can be explained by a bifunctional mechanism for DME oxidation, in which Ru acts as a source of the surface oxidant, most likely H_2O-derived OH species, for the chemisorbed CO intermediate, thus reducing the degree of Pt-site poisoning. However, at extreme cases, i.e., at a high content of the second metal, this beneficial effect is offset by the "dilution" of the Pt sites on the catalyst surface. Particularly, clusters of two to three Pt atoms are required for DME adsorption and its subsequent dehydrogenation. The probability of cluster formation is lowered in the presence of the second metal (e.g., Ru), which, for a high second-metal content, is expected to lead to a change in the RDS from CO oxidation to CO formation [10, 12, 13]. Similar reasoning has been used to explain the optimal PtRu composition for methanol oxidation [14]. In agreement with this interpretation, Liu et al. found that, in spite of decreasing the onset potential of DME

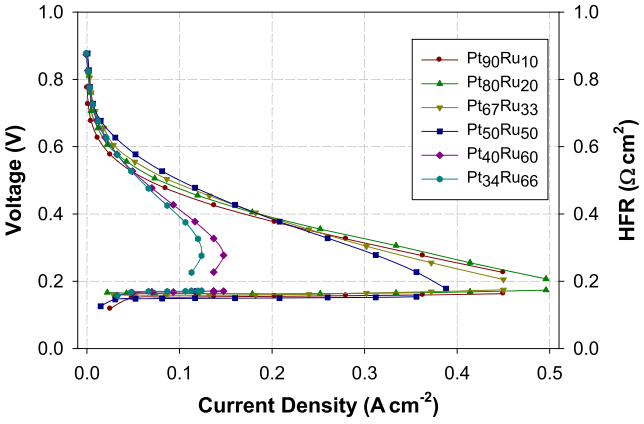

Fig. 1 DDMEFC performance with different PtRu anode catalysts. Anode: 6.0 mg cm^{-2} PtRu black, 40 sccm DME gas, back pressure 2.0 bar; cathode: 4 mg cm^{-2} Pt black, 500 sccm air, back pressure 1.4 bar; membrane Nafion® 117; cell temperature 80 °C

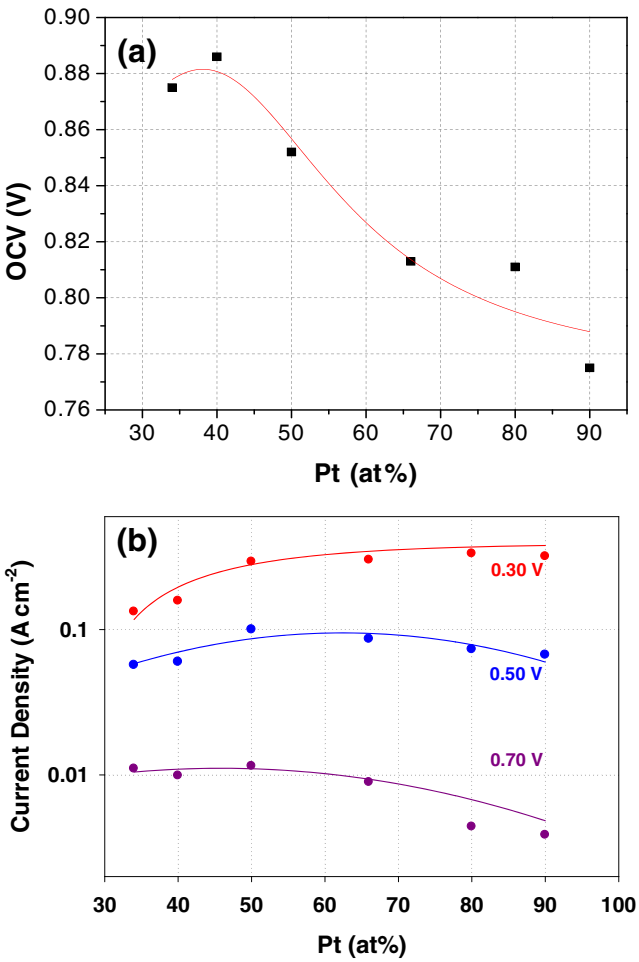

Fig. 2 **a** OCV and **b** DDMEFC current density at different voltages as a function of Pt content in the PtRu catalysts

electrooxidation, the Ru addition resulted in an increase in the activation energy of DME electrooxidation from 46 kJ mol^{-1} on Pt/C to 57 kJ mol^{-1} on PtRu/C [10]. Finding the ideal balance between the need for Pt clusters for DME molecule dehydrogenation and the presence of Ru to oxidize adsorbed CO is likely the key to successful development of a viable DME oxidation electrocatalyst. The need for balancing Pt- and Ru-site content in PtRu catalysts is important for maximizing the activity of methanol oxidation catalysts [15, 16]. While that balance is also important for optimizing performance of catalysts for DME oxidation, the latter process must also take into account the oxidation potential of the catalyst itself (not the case in methanol oxidation catalysts). This makes the selection of the best catalyst for DME oxidation more challenging.

Anode Activity and Fuel Crossover

DME anode polarization plots measured with different PtRu catalysts are presented in Fig. 3. In turn, the onset potential and working potential values at two different current densities of DME oxidation (0.1 and 0.4 A cm^{-2}) are summarized in Table 2. In order to minimize the effect of residual currents on the measured potential value, the onset potential has been defined in this work as the potential at which the current density of DME oxidation reaches 0.01 mA cm^{-2}. In agreement with Fig. 1, Ru-rich catalysts are more active for the DME oxidation at low potentials, below 0.35 V (lower onset potentials of DME oxidation). Pt-rich catalysts perform better at higher potentials, above 0.5 V. The PtRu anodes tend to undergo deactivation towards DME oxidation at even higher potentials (E>0.8 V). The deactivation is more severe for Ru-rich than Pt-rich catalysts. The effect can be ascribed to more facile oxide formation of the surface of Ru-rich catalysts and possibly also due to Ru dissolution [14].

Table 2 DDMEFC anode polarization data obtained with different PtRu catalysts

Catalyst	Onset potentials (V)	E at j=0.1 A cm^{-2} (V)	E at j=0.4 A cm^{-2} (V)
$Pt_{90}Ru_{10}$	0.338	0.412	0.505
$Pt_{80}Ru_{20}$	0.298	0.400	0.496
$Pt_{67}Ru_{33}$	0.278	0.388	0.561
$Pt_{50}Ru_{50}$	0.238	0.374	0.590
$Pt_{40}Ru_{60}$	0.248	0.405	N/A
$Pt_{34}Ru_{66}$	0.230	0.438	N/A

The crossover plots for DME and methanol are compared in Fig. 4. The experiments indicate much lower DME oxidation currents at the cathode than those of methanol, especially at higher potentials, suggesting lower DME crossover and, once again, the inactivity of the oxidized Pt surface (possibly also Ru-contaminated [17]) for DME oxidation. The data show that, unlike the oxidation of methanol, DME oxidation is significantly hindered on the oxide-covered surface of Pt, an effect also observed by Liu et al. [8]. A similar effect can be seen for the PtRu alloy catalysts in Fig. 3.

DDMEFC Performance Optimization

The effect of DME mass transfer on the DDMEFC performance was studied as functions of the flow rates of humidified DME gas and anode back pressure. Panels a and b of Fig. 5 show, correspondingly, the influence of the DME flow rate and anode back pressure on DDMEFC performance. While changing the DME flow rate in the range from 40 to 140 sccm (standard cubic centimeters per minute) has little effect on the

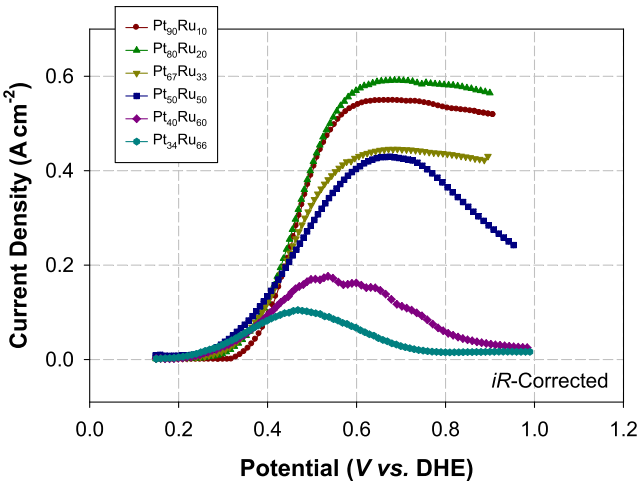

Fig. 3 DDMEFC anode polarization plots. Anode: 6.0 mg cm^{-2} PtRu black, 40 sccm DME, back pressure 2.0 bar; cathode: 4.0 mg cm^{-2} Pt black, back pressure 1.4 bar, 200 sccm H_2; membrane Nafion® 117; cell temperature 80°C

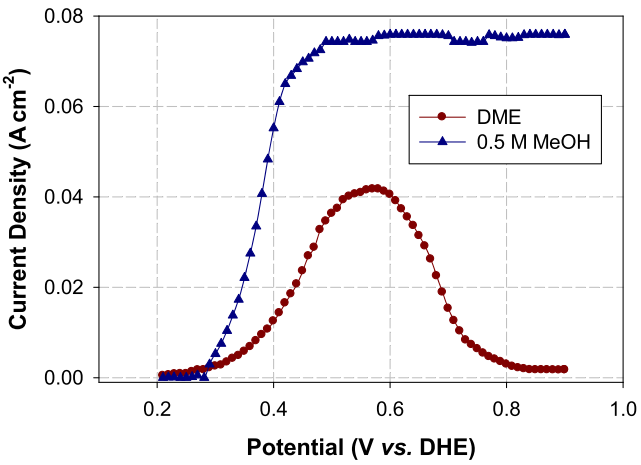

Fig. 4 Fuel crossover plots for a DDMEFC and DMFC. Anode: 6.0 mg cm^{-2} $Pt_{50}Ru_{50}$ black, 40 sccm DME, back pressure 2.0 bar or 0.5 M MeOH, 1.8 mL min^{-1}; cathode: 4.0 mg cm^{-2} Pt black, 200 sccm N_2; membrane Nafion® 117; cell temperature 80°C

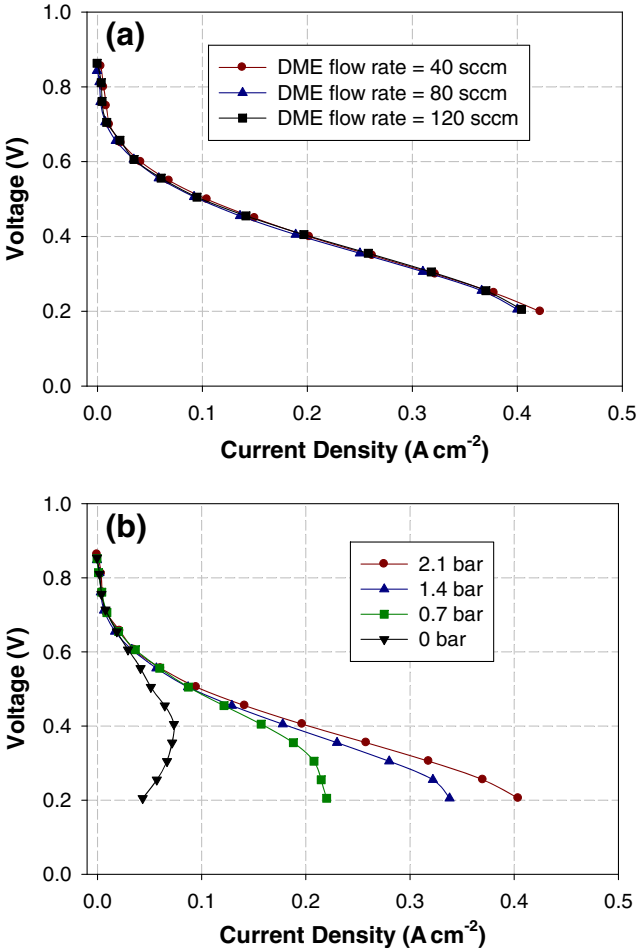

Fig. 5 Effect of **a** DME gas flow rate and **b** anode back pressure on DDMEFC performance. Anode: 6.0 mg cm^{-2} $Pt_{50}Ru_{50}$ black; cathode: 4.0 mg cm^{-2} Pt black, back pressure 1.4 bar, 500 sccm air; membrane Nafion® 117; cell temperature 80 °C

DDMEFC performance, the cell performance in the mass-transport-controlled region is noticeably enhanced by an increase in the anode back pressure from 0 to 2.1 bar.

Recently, using impedance, Ueda et al. [18] demonstrated that anode humidification plays a significant role in the DDMEFC performance. The ideal stoichiometric DME-to-water and methanol-to-water molar ratios in DDMEFC and DMFC oxidation are 1:3 and 1:1, respectively, i.e., the oxidation of DME requires significantly more water than the oxidation of methanol. Anode humidification at 85 °C, which was initially used in this study, yields a DME-to-water molar ratio of approximately 1:0.7. Since this is significantly higher than the stoichiometric ratio of 1:3, water starvation is likely to occur at the anode, lowering the rate of DME electrooxidation. Higher anode humidification temperatures of 95 and 110 °C were therefore used to determine the effect of the water content on the rate of DME oxidation. At these humidification temperatures, the expected DME-to-water molar ratios are 1:0.9 and 1:3, respectively. The measured total pressures of the anode humidifier, DME partial pressures, and corresponding DME-to-water molar ratios at various temperatures are listed in Table 3. As shown in Fig. 6, the cell performance is enhanced when the ideal DME-to-water molar ratio approaches the stoichiometric value of 1:3. The DDMEFC current density at 0.5 V measured with DME-to-water molar ratios of 1:0.7, 1:0.9, and 1:3 are ca. 0.10, 0.12, and 0.14 A cm^{-2}, respectively. Noteworthy, the HFR of the cell is nearly independent of the DME-to-water molar ratio, suggesting that the enhanced DDMEFC performance is not due to an improvement in the ionic conductivity of the membrane but is indeed caused by the effect adjusting the ratio of the two reagents in the initial step of the oxidation process.

Since DME is much less polar than methanol, it is expected to permeate the Nafion® membrane to a lesser degree than methanol. There is, however, conflicting information regarding the effects of DME crossover in the literature. Muller et al. [2] found only trace amounts of CO_2 in the cathode outlet and concluded that DME was not oxidized at the cathode. Mizutani et al. [3] demonstrated that DME had less effect on the oxygen reduction reaction (ORR) than methanol in the half-cell experiments. The permeated DME was not oxidized to the same degree in the DDMEFC as methanol in the DMFC. In contrast, Mench et al. [19] and Herring et al. [20] obtained lower fuel cell performance when using relatively thin Nafion® 115 or 112 membranes in comparison to thick Nafion® 117. Those results suggest a significant impact of DME crossover on the fuel cell performance.

In this work, Nafion® 117 (175 μm thick) and Nafion® 212 (50 μm thick) were used in the DDMEFC testing. The influence of membrane thickness on fuel cell performance is shown in Fig. 7. Unlike DMFC performance, the *iR*-corrected DDMEFC performance in the kinetic region is independent of the membrane thickness, indicating relatively low fuel crossover and/or low activity of DME at the Pt cathode compared to that of methanol (this agrees with the anode polarization data in Fig. 4). In the high current density range, the effect of fuel crossover diminishes due to a decrease in the concentration gradient across the membrane caused by an increased consumption of DME at the anode. Also, the generation of large quantities of water at the cathode may inhibit DME permeation at high current densities [3]. Based on the results of this study, it can be concluded that a thinner membrane

Table 3 Gas pressures and DME-to-water ratios as a function of humidification temperature

Anode humidifier temperature (°C)	Total pressure (kPa)	Water vapor pressure (kPa)	DME partial pressure (kPa)	DME-to-water ratios
85	143	58	85	1:0.7
95	177	85	93	1:0.9
110	191	143	48	1:3.0

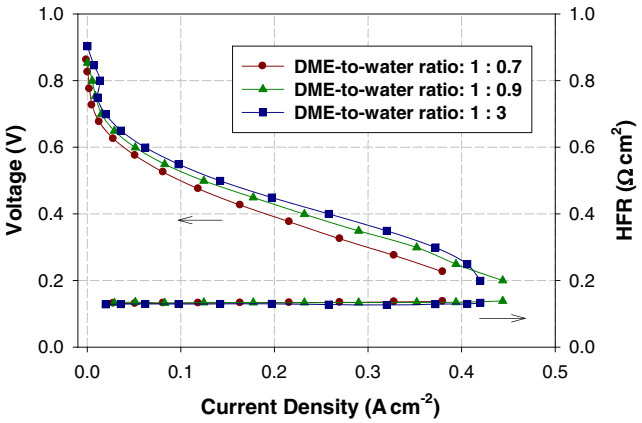

Fig. 6 DDMEFC polarization plots as a function of DME-to-water molar ratios. Anode: 6.0 mg cm^{-2} $Pt_{50}Ru_{50}$ black, 40 sccm DME gas, back pressure 2.0 bar; cathode: 4.0 mg cm^{-2} Pt black, 500 sccm air, back pressure 1.4 bar; membrane Nafion® 117; cell temperature 80 °C

benefits the DDMEFC performance due to a lower ohm resistance without much of a penalty from increased DME crossover. Nafion® 212 membrane was thus used in the DDMEFC experiments described in the section below.

DDMEFC vs. DMFC

Müller et al. [2] demonstrated that performance of a DDMEFC under 5 atm at 130 °C is nearly identical to that of a DMFC. However, the DDMEFC performance remains inferior to that of a DMFC at a more realistic temperature of 80 °C. The performance of an optimized DDMEFC at 80 °C is compared to that of a DMFC in Fig. 8a. The measured performance was summarized in Table 4. Although the anode polarization data in Fig. 8b indicate slower kinetics of DME oxidation compared to that of methanol, the DDMEFC

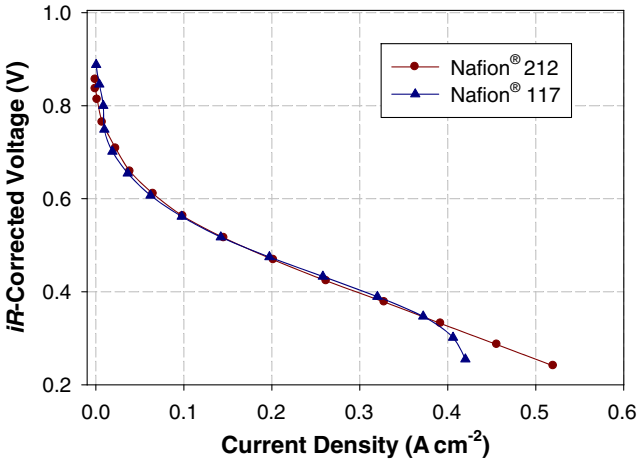

Fig. 7 *iR*-corrected DDMEFC polarization plots recorded with Nafion® 117 and Nafion® 212 membranes. Anode: 6.0 mg cm^{-2} $Pt_{50}Ru_{50}$ black, 40 sccm DME gas, back pressure 2.0 bar, 110 °C anode humidifier; cathode: 4.0 mg cm^{-2} Pt black, 500 sccm air, back pressure 1.4 bar; cell temperature 80 °C

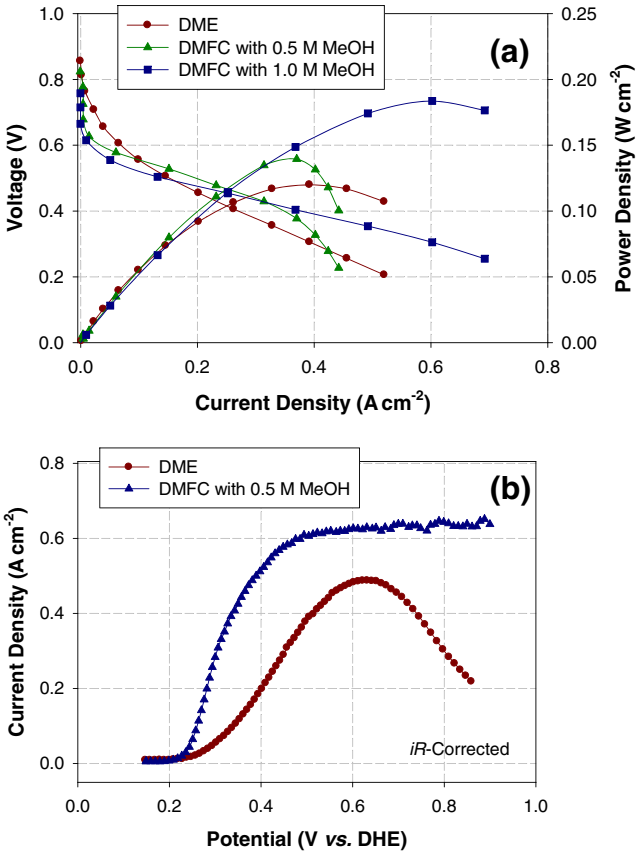

Fig. 8 DDMEFC and DMFC **a** VI and **b** anode polarization plots. Anode: 6.0 mg cm^{-2} $Pt_{50}Ru_{50}$ black, 40 sccm DME gas, back pressure 2.0 bar, 110 °C anode humidifier or 1.8 mL min^{-1} methanol solution, back pressure 0 bar; cathode: 4.0 mg cm^{-2} Pt black, 500 sccm air or 200 sccm H_2, back pressure 1.4 bar; membrane Nafion® 212; cell temperature 80°C

performance is superior to that of the DMFC at cell voltages higher than 0.55 and 0.49 V for two "standard" methanol feed concentrations of 0.5 and 1.0 M, respectively. The effect is most likely caused by the lower fuel crossover and reduced impact on the cathode performance. Furthermore, the DDMEFC OCV values are ca. 32 mV (0.856 vs. 0.824 V) and 98 mV (0.856 vs. 0.758 V) higher than OCV values measured with a DMFC operating on 0.5 and 1.0 M methanol, respectively. A maximum power density of 0.12 W cm^{-2} is achieved at a current density of 0.39 A cm^{-2}. To our best knowledge,

Table 4 Fuel cell performance of optimized DDMEFC and DMFC

	DDMEFC	DMFC (0.5 M)	DMFC (1.0 M)
OCV (V)	0.856	0.824	0.758
j at 0.5 V (A cm^{-2})	0.146	0.196	0.132
Maximum power density (W cm^{-2})	0.120	0.139	0.184
Fuel crossover limiting current (A cm^{-2})	0.136	0.210	0.338

the achieved DDMEFC performance is higher than the best performance published to date [21].

Electrooxidation of DME and methanol on the $Pt_{50}Ru_{50}$ black catalyst was also studied in an electrochemical cell at 25 °C (Fig. 9). In the absence of either DME or methanol in the solution, the voltammetric features in the potential range from 0.05 to 0.40 V are solely reflective of hydrogen adsorption/desorption. In the presence of both fuels, the hydrogen peaks are significantly suppressed by chemisorbed intermediate species, most likely CO. It is worth noting that DME oxidation on the $Pt_{50}Ru_{50}$ catalyst in this work gave rise to a single broad peak (cf. Fig. 9) rather than two peaks observed with Pt catalysts by Kerangueven [7] and Zhang [9] and attributed to the oxidation of CO_{ad} and $(–CHO)_{ad}$. No oxidation current was observed in this work above 0.9 V, where the PtRu surface becomes gradually covered with oxides and therefore less active in the DME oxidation [8, 10]. This is unlike the case of methanol oxidation that continues up to 1.2 V. In contrast with Müller's result [2], the CV curves with and without DME above 0.9 V in the positive-going scan are not completely identical, indicating that some adsorbed species may be present at the Pt surface in this potential region and block the formation of Pt oxides. During the positive-going scan, the onset potential of DME oxidation on the $Pt_{50}Ru_{50}$ catalyst is by ca. 90 mV higher than that of methanol oxidation (0.39 vs. 0.30 V). Furthermore, the current peak of methanol oxidation measured on the $Pt_{50}Ru_{50}$ catalyst is significantly larger than that of DME oxidation. The presented data imply that, in agreement with the anode polarization plots at 80 °C (Fig. 8b), DME does not adsorb and oxidize as readily as methanol on PtRu catalysts at 25 °C. Müller et al. [2] offered two explanations of this effect: (i) C–H bonds in the second methyl group in the DME molecule being less reactive than C–H bonds in methanol and (ii) adsorption of DME on the surface partially covered with CO being less likely than that of methanol.

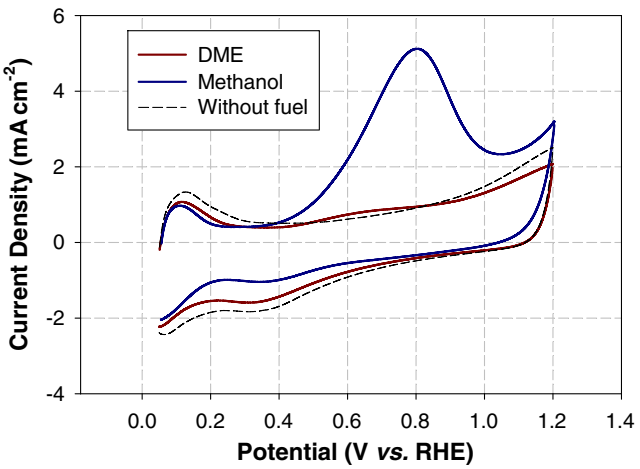

Fig. 9 Cyclic voltammetry of 60 μg cm^{-2} $Pt_{50}Ru_{50}$ black catalyst in 0.1 M $HClO_4$ containing 0.8 M DME or 0.5 M methanol, without any fuel under N_2 atmosphere at room temperature. Scan rate 50 mV s^{-1}

Conclusions

In this work, unsupported PtRu anode catalysts with a wide range of Pt-to-Ru ratios were systematically studied in DDMEFCs. Ru-rich catalysts offer better performance at high fuel cell voltages (kinetic region of the anode), while Pt-rich catalysts perform better at low voltages. $Pt_{50}Ru_{50}$ shows the best overall performance at potentials, where the anode performance is controlled by the rate of DME oxidation. These observations can be explained by a bifunctional mechanism for DME oxidation, whereby the presence of Ru in Pt-based catalysts has two opposing effects. Ru is capable of activating water molecules to generate OH species at low potentials. These surface OH species subsequently act as an oxidant of the adsorbed CO on Pt, likely the dominant intermediate poisoning Pt sites during DME oxidation. In the meantime, high Ru content reduces the probability of Pt cluster formation. Such clusters are required for DME adsorption and subsequent dehydrogenation in the early phase of the oxidation process.

The optimization of fuel cell operation conditions, including DME flow rate, anode back pressure, DME-to-water molar ratio, and membrane thickness, helps maximize the DDMEFC performance. In this work, a maximum power density of 0.12 W cm^{-2} was achieved at a current density of 0.39 A cm^{-2}. Compared to the traditional DMFC, an optimized DDMEFC performs better at cell voltages higher than 0.55 and 0.49 V for 0.5 and 1.0 M methanol feed concentrations, respectively. This is mainly due to a lower crossover and/or lower activity of DME at the air cathode compared to methanol. However, the DME oxidation at PtRu catalysts remains kinetically handicapped relative to methanol. Further development of advanced electrocatalysts for DME oxidation is the key to the success of implementing the DDMEFC technology [22].

Acknowledgments Financial support from the DOE-EERE Fuel Cell Technologies Program (project ID: FC091) is gratefully acknowledged.

Open Access This article is distributed under the terms of the Creative Commons Attribution License which permits any use, distribution, and reproduction in any medium, provided the original author(s) and the source are credited.

References

1. J.O. Jensen, A. Vassiliev, M.I. Olsen, Q.F. Li, C. Pan, L.N. Cleemann, T. Steenberg, H.A. Hjuler, N.J. Bjerrum, J Power Sources **211**, 173 (2012)

2. J.T. Muller, P.M. Urban, W.F. Holderich, K.M. Colbow, J. Zhang, D.P. Wilkinson, J Electrochem Soc **147**, 4058 (2000)
3. I. Mizutani, Y. Liu, S. Mitsushima, K.I. Ota, N. Kamiya, J Power Sources **156**, 183 (2006)
4. A. Serov, C. Kwak, Appl. Catal. B-Environ. **91**, 1 (2009)
5. Y. Tsutsumi, Y. Nakano, S. Kajitani, S. Yamasita, Electrochem. **70**, 984 (2002)
6. M.H. Shao, J. Warren, N.S. Marinkovic, P.W. Faguy, R.R. Adzic, Electrochem Commun **7**, 459 (2005)
7. G. Kerangueven, C. Coutanceau, E. Sibert, F. Hahn, J.M. Leger, C. Lamy, J Appl Electrochem **36**, 441 (2006)
8. Y. Liu, M. Muraoka, S. Mitsushima, K.I. Ota, N. Kamiya, Electrochim Acta **52**, 5781 (2007)
9. Y. Zhang, L.L. Lu, Y.J. Tong, M. Osawa, S. Ye, Electrochim Acta **53**, 6093 (2008)
10. Y. Liu, S. Mitsushima, K. Ota, N. Kamiya, Electrochim Acta **51**, 6503 (2006)
11. J.H. Yoo, H.G. Choi, C.H. Chung, S.M. Cho, J Power Sources **163**, 103 (2006)
12. G. Kerangueven, C. Coutanceau, E. Sibert, J.M. Leger, C. Lamy, J Power Sources **157**, 318 (2006)
13. Q. Li, G. Wu, C. Johnston, P. Zelenay, ECS Trans **41**, 1969 (2011)
14. G. Wu, L. Li, B.-Q. Xu, Electrochim Acta **50**, 1 (2004)
15. H.A. Gasteiger, N. Markovic, P.N. Ross, E.J. Cairns, J Electrochem Soc **141**, 1795 (1994)
16. G. Wu, L. Li, J.-H. Li, B.-Q. Xu, Carbon **43**, 2579 (2005)
17. P. Piela, C. Eickes, E. Brosha, F. Garzon, P. Zelenay, J Electrochem Soc **151**, A2053 (2004)
18. S. Ueda, M. Eguchi, K. Uno, Y. Tsutsumi, N. Ogawa, Solid State Ionics **177**, 2175 (2006)
19. M.M. Mench, H.M. Chance, C.Y. Wang, J Electrochem Soc **151**, A144 (2004)
20. J.R. Ferrell, M.C. Kuo, A.M. Herring, J Power Sources **195**, 39 (2010)
21. J.Y. Im, B.S. Kim, H.G. Choi, S.M. Cho, J Power Sources **179**, 301 (2008)
22. Q. Li, G. Wu, Z.X. Bi, C. Johnston, P. Zelenay, ECS Trans **50**, 1933 (2013)